Modern Physics Letters A

Production of *S*-wave charmonia in the soft gluon resummation approach using the NRQCD

Vladimir Saleev
Samara National Research University, Moskovskoe Shosse, 34, 443086, Samara, Russia

Joint Institute for Nuclear Research, Dubna, 141980 Russia.
saleev.vladimir@gmail.com

Kirill Shilyaev
Samara National Research University, Moskovskoe Shosse, 34, 443086, Samara, Russia.
kirillsept@gmail.com

Received (Day Month Year)
Revised (Day Month Year)

In this article, we study the S-wave charmonium production at the small transverse momenta in the transverse momentum dependent (TMD) parton model (PM), as it is formulated in the soft gluon resummation (SGR) approach, using the nonrelativistic quantum chromodynamics (NRQCD) as the model of the heavy quarkonium hadronization. To extend the scope of the calculation to the phenomenologically important region of intermediate transverse momenta, we use the inverse-error weighting (InEW) matching scheme to combine the TMD PM predictions with the results of the collinear PM (CPM) fixed-order calculations, which are applicable at the large transverse momenta. We predict the direct η_c and the prompt J/ψ production cross sections and transverse momentum spectra in proton-proton collisions at the LHC, RHIC, AFTER and NICA energies. Predictions for the polarized J/ψ production processes are also presented.

Keywords: Quantum chromodynamics; collinear factorization; TMD factorization; charmonium; soft gluon resummation; nonrelativistic QCD.

PACS Nos.: 13.60.Le; 13.88.+e.

1. Introduction

Description of the heavy quarkonium production of mass M in the domain of small transverse momenta, i.e. $p_T \ll M$, is mostly more complicated than the one at the large transverse momenta, $p_T \gg M$, where the collinear parton model (CPM) including the fixed-order perturbative calculation in the quantum chromodynamics (QCD) is the conventional approach.[1] The most adequate approach for the small-p_T kinematical region is the transverse momentum dependent (TMD) parton model (PM).[2,3] In the TMD PM, the soft-hard factorization theorem is originally applied to describe the small-p_T production of the Drell-Yan pairs, W and Z bosons,[4–8]

and Higgs bosons,[9–12] i.e. colorless particles, for which both the final state gluon radiation and the final state soft gluon exchange are absent. In this case, the soft gluon initial radiation and the soft gluon exchange can be factorized in the TMD parton distribution functions (PDFs). The latter ones include dependencies on the initial longitudinal and transverse momenta of the partons and these dependencies are not split up in general. The evolution of TMD PDFs with a factorization scale μ and a rapidity separation scale ζ is controlled by the system of the Collins-Soper-Sterman (CSS) differential equations.[2,13]

Here we study the charmonium production via gluon fusion subprocesses in collisions of unpolarized protons. In general, the unpolarized and linearly polarized gluons may contribute to the production cross section.[14] The contribution in the transverse momentum spectrum of a linearly polarized gluon TMD PDF, the so-called Boer-Mulders PDF, is estimated to be relatively small (10-20%), when it is calculated using the SGR approach[14]. Such a way, we omit this contribution during the presented study.

In order to describe the heavy quark-antiquark pair hadronization into a final heavy quarkonium we use the model of nonrelativistic quantum chromodynamics (NRQCD).[15] The NRQCD includes contributions of color singlet and color octet intermediate states, for the latter ones the soft gluon final state radiation can't be ignored. Formally, TMD factorization can be used but TMD PDFs become process-dependent. As recently shown in Ref.,[16] the proper TMD factorization for quarkonia production requires the introduction of a new non-perturbative hadronic quantities beyond the TMD PDFs: the TMD shape functions. It seems that the use of heavy quarkonium production to probe gluon TMD PDFs is still a very complicated task.

Taking in mind the phenomenological aim of our study, to provide predictions of total cross sections and transverse momentum spectra of S-wave charmonia relevant for future experiments, we use here the well-known soft gluon resummation (SGR) approach[4,17] as a realization of the TMD factorization for modelling of the non-collinear parton dynamics at small transverse momentum of charmonium. In general, our approach is close to the recent studies in Refs.[18,19]

In order to extend the scope of the calculation to the phenomenologically important region of intermediate transverse momenta, we use the inverse-error weighting (InEW) matching scheme[20] to combine the TMD PM predictions and the results of the collinear PM (CPM) fixed-order calculations, which are applicable at the large transverse momenta.

2. Soft gluon resummation approach

The 4-momenta of the initial partons within the TMD PM are taken on-shell $q_{1,2}^2 = 0$ and can be written in the Sudakov decomposition form:

$$q_1^\mu = x_1 p_1^\mu + y_1 p_2^\mu + q_{1T}^\mu, \qquad q_2^\mu = x_2 p_2^\mu + y_2 p_1^\mu + q_{2T}^\mu, \tag{1}$$

where $p_{1,2} = \frac{\sqrt{s}}{2}(1,0,0,\pm 1)$ are 4-momenta of colliding protons, x_i and $y_i = \vec{q}_{iT}^{\,2}/(sx_i)$ are longitudinal fractions of the parton momenta and $\vec{q}_{iT}$ are their transverse momenta ($q_{iT}^2 = -\vec{q}_{iT}^{\,2}$). The TMD factorization prescribes the initial transverse momenta to be small compared to the hard scale of the process μ which is of order of charmonium mass M, so that the corrections of order $\mathcal{O}(\vec{q}_{iT}^{\,2}/M^2)$ are neglected here, and therefore $y_{1,2} \approx 0$. Then the initial 4-momenta are written as follows:

$$q_1 \approx \left(\frac{x_1\sqrt{s}}{2}, \vec{q}_{1T}, \frac{x_1\sqrt{s}}{2}\right), \qquad q_2 \approx \left(\frac{x_2\sqrt{s}}{2}, \vec{q}_{2T}, -\frac{x_2\sqrt{s}}{2}\right). \tag{2}$$

The TMD PM allows, as mentioned above, to describe a production cross section as a convolution of a partonic $2 \to 1$ cross section $d\hat{\sigma}$ and TMD PDFs:[2]

$$d\sigma^{TMD} = \int dx_1\, dx_2\, d^2q_{1T}\, d^2q_{2T}\, F(x_1, \vec{q}_{1T}, \mu, \zeta_1)\, F(x_2, \vec{q}_{2T}, \mu, \zeta_2)\, d\hat{\sigma}^{2\to 1}. \tag{3}$$

The $2 \to 1$ subprocesses of the charmonium $\mathcal{C}$ production with quarks and gluons ($gg \to \mathcal{C}, q\bar{q} \to \mathcal{C}$) are taken into account because they are at leading order at small p_T, the cross section of the corresponding subprocess is

$$d\hat{\sigma}^{2\to 1} = (2\pi)^4 \delta^{(4)}(q_1 + q_2 - p) \frac{\overline{|\mathcal{M}(2\to 1)|^2}}{I} \frac{d^3p}{(2\pi)^3 2p_0} \tag{4}$$

where $I \approx 2x_1x_2s$ is the flux factor and $\mathcal{M}(2 \to 1)$ is the amplitude of a gluon-gluon fusion subprocess $gg \to \mathcal{C}$ or a quark-antiquark annihilation subprocess $q\bar{q} \to \mathcal{C}$, and $\mathcal{C} = \eta_c, J/\psi, \chi_{cJ}, \psi'$. Taking in mind the condition $p_T \ll M$, we can rewrite (4) as follows:

$$\frac{d\hat{\sigma}^{2\to 1}}{dp_T dy} = \frac{2\pi^2 p_T}{sM^2} \overline{|\mathcal{M}(2\to 1)|^2} \delta^{(2)}\left(\vec{q}_1 + \vec{q}_2 - \vec{p}_T\right) \delta\left(x_1 - \frac{Me^y}{\sqrt{s}}\right) \delta\left(x_2 - \frac{Me^{-y}}{\sqrt{s}}\right). \tag{5}$$

In this way, the factorization formula (3) looks like this:

$$\frac{d\sigma^{TMD}}{dp_T dy} = \frac{2\pi^2 p_T}{sM^2} \overline{|\mathcal{M}(2\to 1)|^2} F(x_1, \vec{q}_{1T}, \mu, \zeta) \otimes_T F(x_2, \vec{q}_{2T}, \mu, \zeta), \tag{6}$$

where y is a rapidity of the final quarkonium and

$$F(x_1, \vec{q}_{1T}) \otimes_T F(x_2, \vec{q}_{2T}) = \int d^2q_{1T} d^2q_{2T} F(x_1, \vec{q}_{1T}) F(x_2, \vec{q}_{2T}) \delta^{(2)}(\vec{q}_1 + \vec{q}_2 - \vec{p}_T).$$

The evolution of the TMD PDF with respect to the scales should be implemented after the two-dimensional Fourier transform of the PDF:[2]

$$\hat{F}(x, \vec{b}_T, \mu, \zeta) = \int d^2q_T\, e^{i\vec{q}_T \vec{b}_T} F(x, \vec{q}_T, \mu, \zeta). \tag{7}$$

In terms of the Fourier-conjugated TMD PDFs, we can rewrite the formula (6):

$$\frac{d\sigma^{TMD}}{dp_T dy} = \frac{p_T}{2sM^2} \overline{|\mathcal{M}(2\to 1)|^2} \int d^2b_T e^{-i\vec{b}_T\vec{p}_T} \hat{F}(x_1, \vec{b}_T, \mu, \zeta) \hat{F}(x_2, \vec{b}_T, \mu, \zeta). \tag{8}$$

Within the SGR approach, the perturbative evolution of the Fourier-conjugated PDFs in an impact parameter $\vec{b}_T$ space is implemented in a multiplication way:[21]

$$\hat{F}(x_1, b_T, \mu, \zeta)\hat{F}(x_2, b_T, \mu, \zeta) = e^{-S_P(\mu,\mu_b,b_T)}\hat{F}(x_1, b_T, \mu_b, \mu_b^2)\hat{F}(x_2, b_T, \mu_b, \mu_b^2) \quad (9)$$

where the standard simple choice for the scales $\mu = \sqrt{\zeta}$ was done, and the scale $\mu_0 = \sqrt{\zeta_0} = \mu_b$ was taken as the initial one, the expression for which is given below. This choice is made to minimize large values of the logarithms of the scale ratios $\mu/\Lambda_{\rm QCD}$, μ/M.[22]

In equation (9), the function S_P is the so-called Sudakov factor which realizes the evolution from the initial scales ($\mu_0 = \mu_b, \zeta_0 = \mu_b^2$) to the final ones ($\mu, \zeta = \mu^2$). The Sudakov factor is written this way:[18,21]

$$S_P(\mu, \mu_b, b_T) = \int\limits_{\mu_b^2}^{\mu^2} \frac{d\mu'^2}{\mu'^2}\left[A(\mu')\ln\frac{\mu^2}{\mu'^2} + B(\mu')\right], \quad (10)$$

where the coefficients A and B are presented as a series with respect to the strong coupling constant, and their terms represent logarithmic orders of calculation via $A^{(n)}$ coefficients and orders with respect to the α_s via $B^{(n)}$:

$$A(\mu') = \sum_{n=1}^{\infty} A^{(n)}\left(\frac{\alpha_s(\mu')}{\pi}\right)^n, \qquad B(\mu') = \sum_{n=1}^{\infty} B^{(n)}\left(\frac{\alpha_s(\mu')}{\pi}\right)^n, \quad (11)$$

and the leading logarithmic (LL) and LO in the α_s approximation of the SGR approach (LL-LO) corresponds to the first coefficients of the series

$$A^{(1)} = C_A, \quad (12)$$

$$B^{(1)} = -\frac{11C_A - 2N_f}{6} - \frac{C_A}{2}\delta_{c8}, \quad (13)$$

the quantity δ_{c8} is equal to 0 for color singlet states and 1 for color octet quarkonium states, N_f is a number of quarks flavors, $N_c = 3$ is a number of colors and $C_A = N_c = 3$.

In the one-loop approximation for the coupling constant α_s, an explicit analytical expression for the integral in the function S_P can be obtained.[22] The expression for the Sudakov factor S_P is applicable in the range $b_0/Q \leqslant b_T \leqslant b_{T,\max}$, where $b_0 = 2e^{-\gamma}$, γ is the Euler–Mascheroni constant. The lower limit of the range is given by the expression $\mu_b \to \mu_b' = Qb_0/(Qb_T + b_0)$, and the upper limit[4] is determined by replacing the impact parameter with $b_T \to b_T^*(b_T) = b_T/\sqrt{1 + (b_T/b_{T,\max})^2}$. We used the largest value of the impact parameter $b_{T,\max} = 1.5$ GeV^{-1}. There is some freedom of choice in both the $b_{T,\max}$ parameter and in the form of the b_T prescription; other possible choices and their reasonings can be found in Ref.[22]

In addition, the suppression of the S_P at large b_T is guaranteed by the nonperturbative Sudakov factor S_{NP}, the expression for which is not theoretically derived, so that the function S_{NP} is extracted from experimental data. In the Ref.,[23] the

parameterization in a Gaussian form was obtained for the quark-antiquark annihilation processes:

$$\tilde{S}_{NP}(x, b_T, \mu) = \frac{1}{2}\left[g_1 \ln\frac{\mu}{2Q_{NP}} + g_2\left(1 + 2g_3 \ln\frac{10xx_0}{x_0 + x}\right)\right] b_T^2 \tag{14}$$

with $g_1 = 0.184$ GeV^2, $g_2 = 0.201$ GeV^2, $g_3 = -0.129$, $x_0 = 0.009$, $Q_{NP} = 1.6$ GeV. Due to the lack of experimental data, it is also applied for gluon-gluon fusion processes but with an additional color factor change C_A/C_F,[22] where $C_F = (N_c^2 - 1)/(2N_c) = 4/3$. As two PDFs are included in a cross section expression, we can write the nonperturbative Sudakov factor for the product of the PDFs in this way:

$$S_{NP}(x_1, x_2, b_T, \mu) = \tilde{S}_{NP}(x_1, b_T, \mu) + \tilde{S}_{NP}(x_2, b_T, \mu). \tag{15}$$

In the SGR approach, the TMD PDFs are expressed with collinear parton distributions at the initial scale μ_b' and at the leading order the one can be written as follows:

$$\hat{F}(x, b_T, \mu_b', {\mu_b'}^2) = f(x, \mu_b') + \mathcal{O}(\alpha_s) + \mathcal{O}(b_T \Lambda_{\rm QCD}). \tag{16}$$

They lack the genuine, non-perturbative content, which is a subject of different non-perturbative models of TMD PDFs at the low hard scale, see Refs.[24–27] However, such information is included in the SGR calculations via the non-perturbative Sudakov factor S_{NP} (14). As it will be demonstrated below in Sec. 6, our predictions for η_c production cross sections at the energies 115 GeV and 7 TeV based on the SGR approach coincide with the results obtained earlier in Ref.[28] using the spectator model for non-perturbative gluon TMD PDF, with accuracy about 10-20 %, see Figs. 1 and 2.

Then the master formula for calculation of the differential cross section in the SGR approach reads

$$\frac{d^2\sigma}{dp_T dy} = \frac{\pi p_T \overline{|\mathcal{M}(2 \to 1)|^2}}{M^2 s} \int db_T\, b_T\, J_0(p_T b_T)\; e^{-S_P}\, e^{-S_{NP}}\, f(x_1, \mu_{b*}')\, f(x_2, \mu_{b*}'), \tag{17}$$

where $S_P = S_P(\mu, \mu_{b*}', b_T^*)$ and $S_{NP} = S_{NP}(x_1, x_2, \mu, b_T)$, J_0 is the first kind Bessel function of the zeroth order.

3. Collinear parton model

The relevant LO in the strong coupling constant α_s calculation within the CPM based on the CPM factorization theorem:

$$d\sigma^{CPM} = \int dx_1 \int dx_2\, f(x_1, \mu)\, f(x_2, \mu)\, d\hat{\sigma}(s, x_1, x_2), \tag{18}$$

where $f(x_{1,2}, \mu)$ are gluon (quark and antiquark) collinear PDFs. The partonic cross section is written in the standard way for the $2 \to 2$ subprocesses:

$$d\hat{\sigma} = (2\pi)^4 \delta^{(4)}(q_1 + q_2 - p - k) \frac{\overline{|\mathcal{M}(2 \to 2)|^2}}{I} \frac{d^3p}{(2\pi)^3 2p_0} \frac{d^3k}{(2\pi)^3 2k_0}. \tag{19}$$

Combining (18) and (19) together, we find the basic formula for the numerical calculation in the CPM:

$$\frac{d\sigma^{CPM}}{dydp_T} = \frac{p_T}{8\pi s}\int\frac{dx_1}{x_1}\int\frac{dx_2}{x_2}\,f(x_1,\mu)\,f(x_2,\mu)\,\overline{|\mathcal{M}(2\to 2)|^2}\delta\left(\hat{s}+\hat{t}+\hat{u}-M^2\right), \tag{20}$$

where $\hat{s}=x_1x_2s$, $\hat{t}=M^2-\sqrt{s}M_Te^{-y}$, $\hat{u}=M^2-\sqrt{s}M_Te^{y}$, and $M_T=\sqrt{M^2+p_T^2}$. Considering only the LO contributions from gluon-gluon fusion and quark-antiquark annihilation partonic subrocesses, we included in the LO CPM calculation the next ones: $gg\to\mathcal{C}g$ and $q\bar{q}\to\mathcal{C}g$, where $\mathcal{C}=J/\psi,\eta_c,\chi_{cJ},\psi'$.

In the LO CPM calculations, as well as in the calculations based on the SGR approach, to describe the prompt J/ψ production data, we calculate the sum of the direct production cross section and the feed-down contributions from decays $\chi_{cJ}\to J/\psi\gamma$ and $\psi'\to J/\psi X$.

4. Nonrelativistic QCD

The nonrelativistic QCD (NRQCD) is a conventional approach for the description of the hadronization of heavy quark-antiquark pair into heavy quarkonium.[15] The large mass of the charm quarks m_c allows us to consider them as nonrelativistic ($v^2\approx 0.3$)[29,30], and therefore the following dynamical observables: quarkonium mass, momentum, kinetic energy, etc., are quite reliably separated by orders of their magnitudes.[31] The estimation of the magnitude of observables gives the right to introduce a hierarchy of Fock states of charmonium in the J/ψ production with respect to the relative velocity v of the constituent quarks:[32]

$$|J/\psi\rangle = \mathcal{O}(v^0)|c\bar{c}[^3S_1^{(1)}]\rangle + \mathcal{O}(v^1)|c\bar{c}[^3P_J^{(8)}]g\rangle + \\ + \mathcal{O}(v^2)|c\bar{c}[^3S_1^{(1,8)}]gg\rangle + \mathcal{O}(v^2)|c\bar{c}[^1S_0^{(8)}]g\rangle + \dots \tag{21}$$

The corresponding expansion for the η_c state looks as follows:

$$|\eta_c\rangle = \mathcal{O}(v^0)|c\bar{c}[^1S_0^{(1)}]\rangle + \mathcal{O}(v^1)|c\bar{c}[^1P_1^{(8)}]g\rangle + \\ + \mathcal{O}(v^2)|c\bar{c}[^3S_1^{(1,8)}]g\rangle + \mathcal{O}(v^2)|c\bar{c}[^1S_0^{(1,8)}]gg\rangle + \dots \tag{22}$$

and for P-wave charmonia χ_{cJ} it is

$$|\chi_{cJ}\rangle = \mathcal{O}(v^0)|c\bar{c}[^3P_J^{(1)}]\rangle + \mathcal{O}(v^1)|c\bar{c}[^3S_1^{(8)}]g\rangle + \dots \tag{23}$$

The leading term of the series is the color singlet Fock state, in which the constituent quarks are in the observable charmonium. If we keep only this term, then this approximation is called the Color Singlet Model (CSM).[33]

In the NRQCD, the production cross section of a charmonium state is factorized into the cross section of a quark-antiquark pair production in some Fock state and a long-distance matrix element (LDME), which can be interpreted as describing the hadronization of a quark-antiquark pair into a bound state:

$$d\hat{\sigma}(a+b\to\mathcal{C}+X) = \sum_n d\hat{\sigma}(a+b\to c\bar{c}[n]+X)\langle\mathcal{O}^{\mathcal{C}}[n]\rangle/(N_{\rm col}N_{\rm pol}), \tag{24}$$

where the short notation $n = {}^{2S+1}L_J^{(1,8)}$ denotes the Fock state in the color singlet $^{(1)}$ or color octet $^{(8)}$ state, with spin S, orbital momentum L, total angular momentum J, $N_{\rm pol} = 2J+1$, $N_{\rm col} = 2N_c$ for color singlets, $N_{\rm col} = N_c^2 - 1$ for color octets, and $N_c = 3$. The amplitude of the quark-antiquark pair production in the respective Fock state is calculated in the fixed-order of the perturbative QCD using the Feynman diagram technique and a sequence of projections onto states with the necessary values of the quantum numbers.[15,32]

In the SGR approach, we take into account the production of states ${}^1S_0^{(8)}$, ${}^3P_{0,2}^{(8)}$ for J/ψ; ${}^3P_{0,2}^{(1)}$, ${}^3S_1^{(8)}$ for χ_{cJ}; ${}^1S_0^{(1)}$ for η_c (as the CSM approximation is sufficient and color octet states lead to an overestimation of the experimental data) in subprocesses $2 \to 1$. In the CPM, the charmonia in $2 \to 2$ partonic subprocesses are produced via the states ${}^3S_1^{(1)}$, ${}^3S_1^{(8)}$, ${}^1S_0^{(8)}$ and ${}^3P_J^{(8)}$ for J/ψ, ψ' and via ${}^3P_J^{(1)}$, ${}^3S_1^{(8)}$ for χ_{cJ} . The hard squared matrix elements of heavy quarkonium production in the gluon-gluon fusion and quark-antiquark annihilation corresponding to the color singlet states can be found in Ref.,[34] and those for the color octet states are in Ref.[35]

Nowadays, all known sets of LDME values are phenomenological. The expressions for the color singlet LDMEs are related to the values of the charmonium wave function or its derivative at the origin.[29,30] These values are obtained in calculations in nonrelativistic potential model with phenomenological potentials or from experimental data for charmonium decays. The LDME for color octet states can't be calculated in the QCD and therefore they are extracted by fitting charmonium data after subtraction of the color singlet contributions. Although the LDME values are assumed to be universal, the results of LDME fits of different data sets with various $\sqrt{s}$ and, especially, in different orders of α_s calculations can differ quite significantly. Therefore, in this study we obtain our own results for octet LDMEs by the fitting of prompt J/ψ production data at $\sqrt{s} = 200$ GeV.[36–39]

The η_c production cross sections in proton-proton collisions are measured only in experiments of the LHCb collaboration[40,41] at the $\sqrt{s} = 7$ and 8 TeV, and at the region of applicability of the CPM, $6.5 < p_T^{\eta_c} < 14$ GeV. As it was shown in Ref.,[42] the CPM using the CSM calculation may be sufficient for a correct and complete description of the η_c production cross section and p_T-spectrum. The similar results have been obtained in the calculations based on the high-energy factorization approach and the CSM, see Refs.[43,44]

5. Matching scheme

For the region of intermediate transverse momenta $p_T \sim M$, there is no approach based on the perturbative expansion of the cross section in a series and its representation in the factorized form, as it is done by the collinear and TMD factorization theorems. Instead, the contributions of the two factorization approaches can be matched and, in this way, can describe the intermediate region of p_T as a certain sum of the CPM and TMD PM contributions. We use the Inverse-Error Weighting (InEW) scheme, which is based on the inverse-variance weighting scheme for the

evaluation of the weighted average, such a method for choice of weights for random variables that the variance of their weighted sum is the smallest.[20]

In the InEW scheme, the matched $\overline{d\sigma}$ cross section is represented as the sum of the TMD PM contribution TMD and the collinear fixed-order term CPM with the weights ω_1 and ω_2:

$$\overline{d\sigma}(p_T, Q) = \omega_1\, d\sigma^{TMD}(p_T, Q) + \omega_2\, d\sigma^{CPM}(p_T, Q). \tag{25}$$

The normalized values of the inverse squares of the power corrections used in the CPM and TMD PM are taken as the weights:

$$\omega_1 = \frac{\Delta_{TMD}^{-2}}{\Delta_{TMD}^{-2} + \Delta_{CPM}^{-2}}, \qquad \omega_2 = \frac{\Delta_{CPM}^{-2}}{\Delta_{TMD}^{-2} + \Delta_{CPM}^{-2}}, \tag{26}$$

$$\Delta_{TMD} = \left(\frac{p_T}{Q}\right)^2 + \left(\frac{m}{Q}\right)^2, \qquad \Delta_{CPM} = \left(\frac{m}{p_T}\right)^2 \cdot \left(1 + \ln^2\left(\frac{Q_T}{p_T}\right)\right), \tag{27}$$

where m is a hadronic mass scale of order 1 GeV, $Q_T = \sqrt{Q^2 + p_T^2}$. During our calculations $Q = M$ is the charmonium mass. The uncertainty of the cross section evaluation, defined as the weighted average of the TMD PM and CPM contributions, is given by the following expression:

$$\Delta\overline{d\sigma} = \frac{\Delta_{TMD}\Delta_{CPM}}{\sqrt{\Delta_{TMD}^2 + \Delta_{CPM}^2}}\overline{d\sigma}. \tag{28}$$

Thus, the InEW scheme allows us to calculate a cross section that is reduced to the contributions of the CPM and TMD PM in their regions of applicability and which is represented as a weighted average of these contributions in the region where neither theorem is strictly applicable. The error of the final cross section is found to be of the maximum value in the region of intermediate transverse momenta.

6. Results

All numerical calculations described below were performed using the numerical integrator CUBA[45] with a maximum relative error of 1%. The collinear PDFs were taken as numerically defined distributions MSTW2008LO.[46]

The masses[47] of the charmonium states used in the calculations are $M_{J/\psi} = 3.096$ GeV, $M_{\psi'} = 3.686$ GeV, $M_{\chi_{c0}} = 3.415$ GeV, $M_{\chi_{c1}} = 3.510$ GeV, $M_{\chi_{c2}} = 3.556$ GeV, $M_{\eta_c} = 2.984$ GeV. The branching fractions[47] of charmonium states into lower-energy states and J/ψ branching fractions into lepton pairs are $\mathrm{Br}(\chi_{c0} \to J/\psi + \gamma) = 0.014$, $\mathrm{Br}(\chi_{c1} \to J/\psi + \gamma) = 0.343$, $\mathrm{Br}(\chi_{c2} \to J/\psi + \gamma) = 0.19$, $\mathrm{Br}(\psi' \to J/\psi + X) = 0.614$, $\mathrm{Br}(J/\psi \to e^+e^-) = 0.05971$, $\mathrm{Br}(J/\psi \to \mu^+\mu^-) = 0.05961$. For color singlet states the following LDMEs[48] were used: $\langle \mathcal{O}^{J/\psi}[^3S_1^{(1)}]\rangle = 1.3$ GeV^3, $\langle \mathcal{O}^{\psi'}[^3S_1^{(1)}]\rangle = 0.65$ GeV^3, $\langle \mathcal{O}^{\chi_{c0}}[^3P_0^{(1)}]\rangle = 0.089$ GeV^5 and $\langle \mathcal{O}^{\eta_c}[^1S_0^{(1)}]\rangle = 0.44$ GeV^3.

We make matching of the CPM and TMD PM contributions for description of the charmonium production at arbitrary values of charmonium transverse momentum. The transverse mass of charmonium $M_T = \sqrt{M^2 + p_T^2}$ in the CPM calculations and the mass of charmonium M in the SGR approach were used as scales of factorization, μ, and renormalization, μ_R. In order to calculate the feed-down contributions to the prompt J/ψ production of the kind $\mathcal{C}' \to \mathcal{C} + X$ correctly, the transverse momentum shift effect was taken into account: $p_{T\mathcal{C}} \approx (M_{\mathcal{C}}/M_{\mathcal{C}'}) \cdot p_{T\mathcal{C}'}$.

6.1. η_c production

First, we will consider the η_c production as a clearer case. Here we provide estimations for the η_c production at small p_T where the color singlet state contribution ${}^1S_0^{(1)}$ is the LO of the NRQCD series. That's why, in contrast to the J/ψ production case, there is no need to seek a source of the color octet LDMEs in order to fit them, which is a generally problematic task due to the narrow fitting region $p_T \ll M$ in the TMD PM. In any case, there is no data available for the η_c hadroproduction at the small p_T values. For η_c we can only make theoretical predictions for the color singlet contribution with a known color singlet LDME.

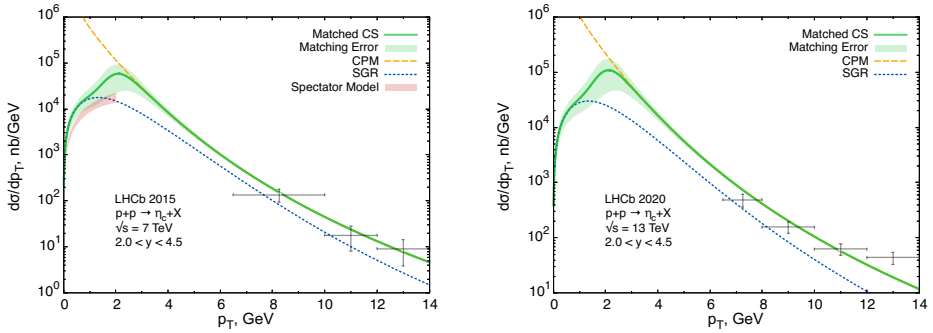

Fig. 1. The cross section of the η_c production as a function of transverse momentum for forward rapidity region $2 < y < 4.5$ at the energies $\sqrt{s} = 7$ TeV (left panel) and 13 TeV (right panel). The spectator model prediction is from Ref.[28] The data are from the LHCb Collaboration[40,41]

The predictions for the η_c production cross section in the LL-LO accuracy are shown in Fig. 1 for the LHCb energies of $\sqrt{s} = 7$ and 13 TeV.[40,41] At first, it is interesting that the LO CPM using the CSM calculation does not contradict LHCb data with respect to the NLO CPM using CSM calculation,[42] which overestimates LHCb data a little when the value $\langle \mathcal{O}^{\eta_c}[{}^1S_0^{(1)}] \rangle = \frac{1}{3}\langle \mathcal{O}^{J/\psi}[{}^3S_1^{(1)}] \rangle \simeq 0.44$ GeV^3 is used. The next surprising finding is a good agreement of the SGR calculation with the data up to $p_T \simeq 14$ GeV. It looks as an artifact of the SGR approach, which should only be applicable in the region of small $p_T < M_{\eta_c}$. In any case, the matched cross section in this region of the transverse momenta p_T is defined by the CPM contribution only.

In Fig. 2, our predictions for the η_c production differential cross sections within the matched SGR plus CPM approach at the $\sqrt{s} = 27$ GeV for the future SPD NICA[49] and at the $\sqrt{s} = 115$ GeV for the AFTER@LHC experiments[50] are presented.

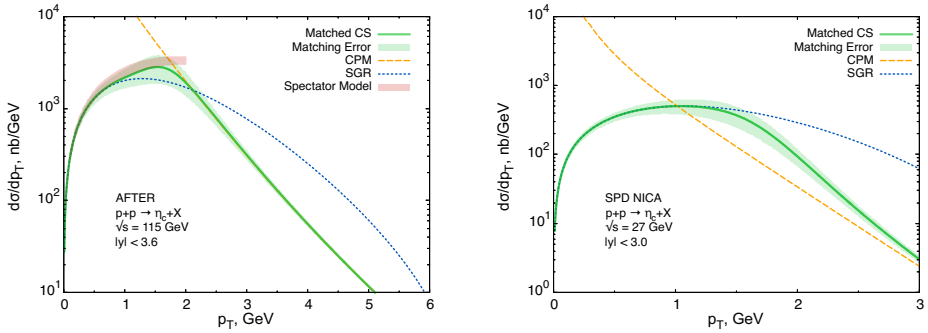

Fig. 2. The cross section of the η_c production as a function of transverse momentum at the energies $\sqrt{s} = 115$ GeV (left panel) and $\sqrt{s} = 27$ GeV (right panel). The spectator model prediction is from Ref.[28]

In Figs. 1 and 2, the predictions obtained in the TMD approach using the spectator model[28] for gluon PDF at the low initial scale are also presented to compare at the region of small transverse momenta $p_T < 2$ GeV. The unpolarized gluon TMD PDF and the Boer-Mulders one were used in terms of the PVGlueModel20 model of Ref.[24] at the initial scale. Their evolution is controlled by the standard Collins-Soper-Sterman equations.[2] We find rather good agreement at the energy $\sqrt{s} = 115$ GeV and our prediction sufficiently overestimates the result of Ref.[28] at the energy $\sqrt{s} = 7$ TeV. Note, according to Ref.,[28] the contribution of the Boer-Mulders function in the η_c production cross sections is about a few percent and the one may be neglected in our predictions.

6.2. *J/ψ production*

The J/ψ production is a more sophisticated sample for test of factorization approaches. As opposed to the η_c hadroproduction at the small transverse momenta, when the gluon-gluon fusion is absolutely dominant contribution, the quark-antiquark annihilation contribution to the J/ψ production cannot be neglected and it is estimated to be about 10% of the total cross section at the $\sqrt{s} = 200$ GeV and it is about $20 - 30\%$ at smaller energies.[51] In this paper, we take into consideration quark-antiquark annihilation subprocesses both in the SGR approach and in the CPM calculation.

We do not take into account the contribution of the octet states ψ' to the prompt production of J/ψ because of their very small value compared to the contributions of the analogous states of J/ψ and their almost identical dependence on p_T in the

LDME fitting in the available domains, since both contributions are described by the same hard amplitudes. One can consider the small octet contributions ψ' to be effectively included in the direct production of the corresponding J/ψ states.

The fit of the octet LDMEs was performed with the experimental data sets of the PHENIX[36,37] and STAR[38,52] collaborations for the J/ψ production in proton–proton collisions at $\sqrt{s} = 200$ GeV in different rapidity intervals, commonly in the SRG ($p_T < 1$ GeV) and in the CPM ($p_T > 5$ GeV) applicability domains under assumption of independence of the LDMEs from the factorization model. The identical dependence on p_T of the ${}^1S_0^{(8)}$ and ${}^3P_J^{(8)}$ contributions to the J/ψ direct production does not allow us to separately extract the corresponding LDMEs within the only one factorization model, so their values are usually obtained only as a linear combination, however, the common fit in the CPM and in the SGR, where the LDMEs are included in two different linear combinations, makes it possible to find both $\langle \mathcal{O}^{J/\psi}[{}^1S_0^{(8)}] \rangle$ and $\langle \mathcal{O}^{J/\psi}[{}^3P_0^{(8)}] \rangle$ separately. In addition, the relations between the LDMEs due to the heavy quark spin symmetry in the leading v order of the NRQCD were used: $\langle \mathcal{O}^{\mathcal{C}}[{}^3P_J^{(8)}] \rangle = (2J+1) \cdot \langle \mathcal{O}^{\mathcal{C}}[{}^3P_0^{(8)}] \rangle$.

The values of the octet LDMEs obtained by fitting the experimental data are in Table 1, where the uncertainties correspond to one standard deviation. The ME for the ${}^3S_1^{(8)}$ states of J/ψ and χ_{cJ} is obviously the same and that follows a zero value of the LDME and an inability of the corresponding LDME extraction due to the close p_T-dependence of these states' cross section up to $p_T \simeq 9$ GeV. More data for large p_T at not very high energies may provide an opportunity to separate them.

The results of cross section calculations for the kinematics of the PHENIX[36] and STAR[52] experiments are plotted in Figs. 3, 4, 5 together with their normalized spectra. Theoretical calculations for the 2007 PHENIX experimental data set[37] are not shown here, since they fully coincide with those in Fig. 3 and 4. The light green bands in the plots show the uncertainties of the cross section within the matching procedure.

Table 1. Result for LDMEs fitting on J/ψ production within domains of $p_T < 1$ GeV (SGR) and $p_T > 5$ GeV (CPM).

$\langle \mathcal{O}^{J/\psi}[{}^1S_0^{(8)}] \rangle$, GeV^3	$(8.73 \pm 0.40) \cdot 10^{-2}$
$\langle \mathcal{O}^{J/\psi}[{}^3P_0^{(8)}] \rangle$, GeV^5	$(2.35 \pm 1.48) \cdot 10^{-3}$
$\langle \mathcal{O}^{J/\psi}[{}^3S_1^{(8)}] \rangle$, GeV^3	$(7.33 \pm 1.22) \cdot 10^{-3}$
$\langle \mathcal{O}^{\chi_{c0}}[{}^3S_1^{(8)}] \rangle$, GeV^3	$(0.00 \pm 1.63) \cdot 10^{-3}$
χ^2/n.d.f.	1.38

Additional uncertainties in the cross section predictions are introduced by the choice of a hard scale and the LDME variations. However, these uncertainties almost disappear when the normalized spectra are calculated. The plots below show, in addition to the main theoretically predicted differential cross sections, also the curves while varying different scales by a factor of 2. The LDME uncertainty hardly

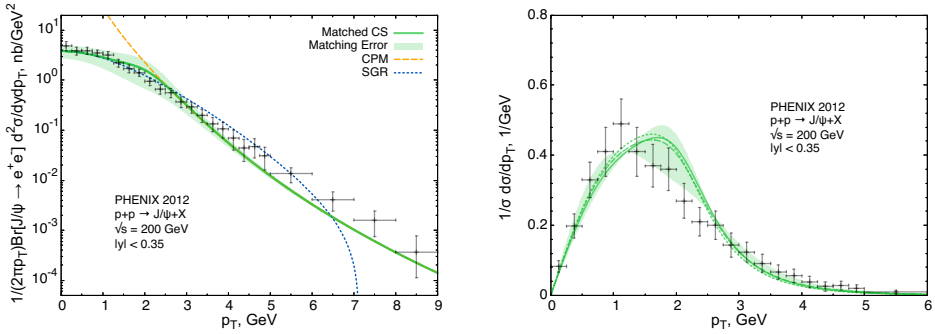

Fig. 3. The cross section of the J/ψ production as a function of transverse momentum at the energy $\sqrt{s} = 200$ GeV and $|y| < 0.35$ (left panel), and the corresponding normalized spectrum (right panel). The data are from the PHENIX Collaboration.[36]

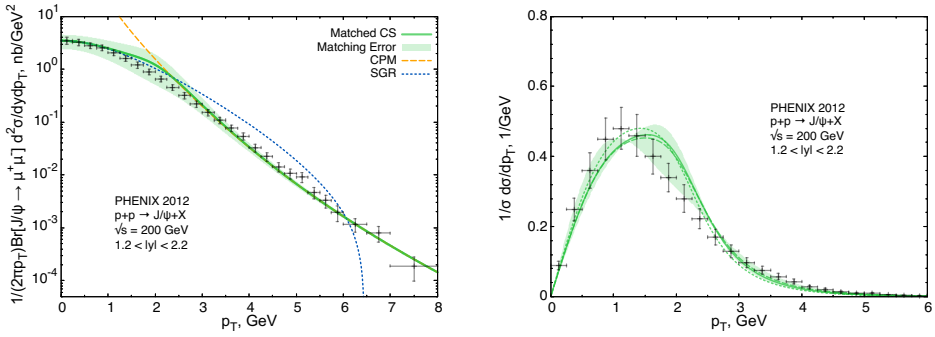

Fig. 4. The cross section of the J/ψ production versus transverse momentum at the PHENIX energy of $\sqrt{s} = 200$ GeV and $1.2 < |y| < 2.2$ (left panel), and the corresponding normalized spectrum (right panel). The data are from the PHENIX Collaboration.[37]

influence on the shape of the spectrum curves, so it cannot be seen on the plots.

Our calculations show that the contribution of the quark-antiquark annihilation subprocesses for the central and middle intervals of rapidity at $\sqrt{s} = 200$ GeV is about 8%, and the feed-down contribution from the $\chi_{cJ} \to J/\psi + \gamma$ decays is only about 4%, while the experimental estimation for the P-wave contributions is about 30%. This contradiction requires a special investigation.

We present predictions for the J/ψ production in the SPD NICA kinematics at $\sqrt{s} = 27$ GeV with the fitted LDMEs. As can be seen in Fig. 6, as the energy $\sqrt{s}$ decreases, the transition region from one factorization to another shifts towards the smaller values of p_T. The estimated contribution of quark-antiquark subprocesses is less than 10%, the fraction of χ_{cJ} decays is about 5%.

Theoretical predictions based on different factorization approaches and different hadronization models are very sensitive to the production of the polarized of J/ψ mesons. It refers to the so-called "quarkonium polarization puzzle", which implies

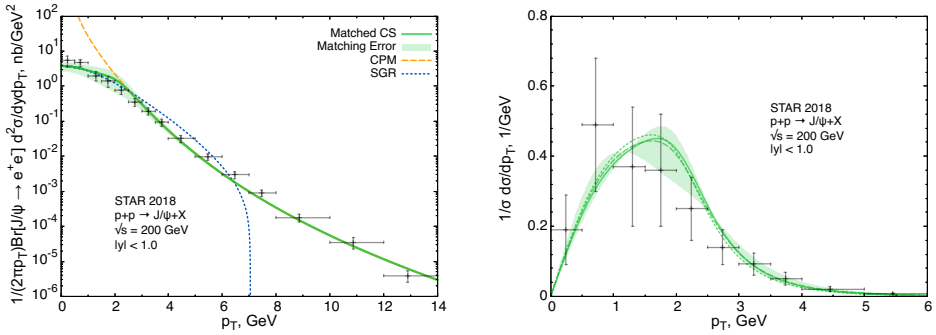

Fig. 5. The cross section of the J/ψ production as a function of transverse momentum at the energy $\sqrt{s} = 200$ GeV and $|y| < 1.0$ (left panel), and the corresponding normalized spectrum (right panel). The data are from the STAR Collaboration[38,52]

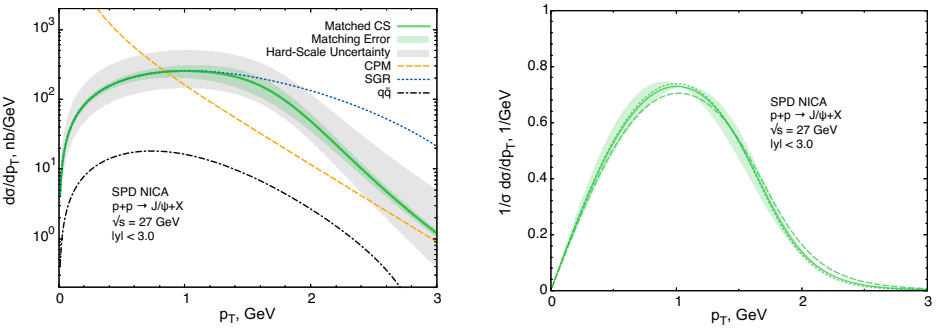

Fig. 6. The cross section of the J/ψ production as a function of transverse momentum at the NICA energy of $\sqrt{s} = 27$ GeV (left panel), and the corresponding normalized spectrum (right panel).

a discrepancy between experimental data and current predictions of the polarized J/ψ production cross sections. At the considered center-of-mass energy, we can analyze the J/ψ polarization data[39] of the PHENIX collaboration for $p_T \leq 5$ GeV to compare with. The data are provided in the helicity frame, where the axis of the longitudinal polarization is directed along the three-dimensional momentum of the J/ψ. To calculate polarized direct J/ψ cross section we should only know that the vector of J/ψ longitudinal polarization in the helicity frame of the J/ψ can be written in the following way:[53]

$$\varepsilon_\mu(J_z = 0) = \frac{(pQ)p_\mu/M - MQ_\mu}{\sqrt{(pQ)^2 - sM^2}}, \tag{29}$$

where p is the J/ψ 4-momentum, Q is the sum of the initial proton's 4-momenta and $s = Q^2$. To calculate the feed-down contribution in the prompt polarized J/ψ production cross section, we need the known polarization tensors for the P-wave

states, which can be obtained by summing the products of the vectors $\varepsilon_\mu(J_z)$ and the corresponding Clebsch–Gordan coefficients:

$$\varepsilon^{(J)}_{\mu\nu}(J_z) = \sum_{J_{1z},J_{2z}} C^{JJ_z}_{J_1 J_{1z},J_2 J_{2z}} \varepsilon_\mu(J_{1z})\varepsilon_\nu(J_{2z}). \tag{30}$$

The explicit NRQCD scheme and relevant formulae for calculation of polarized J/ψ cross section due to the feed-down decays of χ_{cJ} and ψ' can be found in Ref.[54]

We calculate the coefficient λ, which is one of the angular coefficients in the lepton angular distribution in $J/\psi \to l\bar{l}$ decay. This coefficient is expressed in terms of the polarized (L for longitudinal and T for transverse polarization) cross sections:

$$\lambda = (\sigma_T - 2\sigma_L)/(\sigma_T + 2\sigma_L). \tag{31}$$

The comparison of the experimental data with the calculation results is given in Fig. 7, where the channels of direct J/ψ production and χ_{cJ} states decays are shown separately as well. We find good agreement of the calculation with the data at small p_T, the application domain of the TMD factorization theorem, and disagreement within the intermediate $p_T \sim M$ region where the prediction is made using the matching InEW scheme. The polarization of the J/ψ is described with the direct production predominantly, though the channel of the P-wave states decays could describe polarization at $p_T > M$. This may be an evidence for biased fitting of LDMEs for χ_{cJ}, so a more precise description of the χ_{cJ} production could fix both the prediction of polarization at intermediate p_T and the problem of P-wave states fraction in unpolarized J/ψ production which was mentioned above.

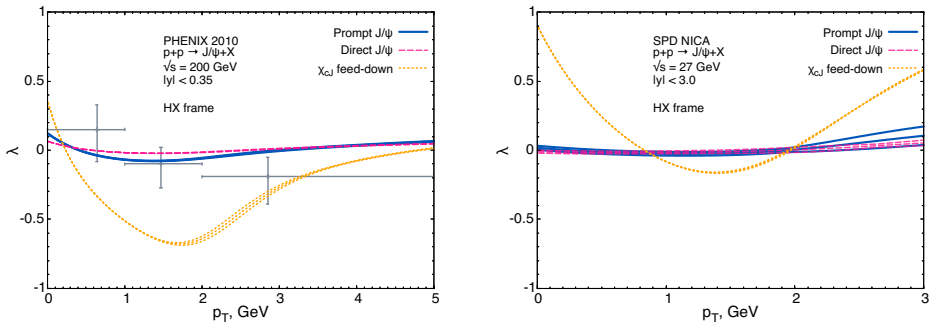

Fig. 7. The angular coefficient λ for J/ψ production within the helicity frame as a function of transverse momentum at the energy $\sqrt{s} = 200$ GeV, $|y| < 0.35$ for PHENIX (left panel) and at the energy $\sqrt{s} = 27$ GeV, $|y| < 3.0$ for SPD NICA (right panel). The data are from the PHENIX Collaboration.[39]

7. Conclusion

In the present paper, we studied the prompt production of S-wave states of charmonium, these are J/ψ and η_c, within the SGR approach as a TMD PM factorization

framework. This TMD PM allows to describe the charmonium production cross section at small p_T and provides the description of the transverse momentum spectrum at moderate and large p_T within the fixed-order CPM calculation using the InEW scheme for matching the SGR approach and CPM.

Firstly, we provide calculations for η_c production within the CSM at the LL-LO accuracy of the SGR approach matched with the LO CPM calculations for energies of present and future experiments: LHCb at $\sqrt{s} = 13$ TeV, AFTER@LHC at $\sqrt{s} = 115$ GeV and SPD NICA at $\sqrt{s} = 27$ GeV. Secondly, we calculate the prompt J/ψ production cross sections at the energy $\sqrt{s} = 200$ GeV (PHENIX, STAR) and at $\sqrt{s} = 27$ GeV (SPD NICA) at LL-LO approximation of the SGR, matched with the LO CPM calculation using the NRQCD. We obtained the color octet LDMEs by fitting them to the experimental data at the $\sqrt{s} = 200$ GeV and used them for prediction of cross section for the SPD NICA energy. We estimate feed-down fraction as well as the relative role of the gluon-gluon fusion and the quark-antiquark annihilation subprocesses in the prompt J/ψ production at the different energies. Thirdly, we describe the PHENIX data for polarized prompt J/ψ production in the helicity frame at the energy $\sqrt{s} = 200$ GeV and $p_T < M$, and make prediction for the future SPD NICA experiment. For both kinematic conditions, J/ψ are predicted to be nearly unpolarized for all p_T value, although this result is in agreement with the PHENIX data at small p_T.

Thus, we demonstrate the relevance of the combined scheme based on the matching between the SGR approach and the fixed-order CPM for the calculation of J/ψ and η_c production cross sections. We should note that the calculation in the NLL-NLO approximation of the SGR approach and at the NLO level of the fixed-order CPM look more accurate and should be made in the future. However, the LDMEs used in the calculations should be redefined appropriately to describe the data. After this, the new theoretical predictions should be very close to those obtained within the present approximations.

8. Acknowledgments

We are grateful to Alexey Guskov, Oleg Teryaev and other members of the SPD NICA Collaboration for a fruitful discussion of the obtained results. The work is supported by the Foundation for the Advancement of Theoretical Physics and Mathematics BASIS, grant No. 24-1-1-16-5, and by the grant of the Ministry of Science and Higher Education of Russian Federation, No. FSSS-2025-0003.

References

1. E. Chapon *et al.*, *Prog. Part. Nucl. Phys.* **122**, 103906 (2022), `arXiv:2012.14161 [hep-ph]`.
2. J. Collins, *Foundations of Perturbative QCD* (Cambridge University Press, 2011).
3. R. Boussarie *et al.* (4 2023), `arXiv:2304.03302 [hep-ph]`.
4. J. C. Collins, D. E. Soper and G. F. Sterman, *Nucl. Phys. B* **250**, 199 (1985).

5. V. Moos, I. Scimemi, A. Vladimirov and P. Zurita, *JHEP* **05**, 036 (2024), arXiv:2305.07473 [hep-ph].
6. A. Bacchetta, G. Bozzi, M. Radici, M. Ritzmann and A. Signori, *Phys. Lett. B* **788**, 542 (2019), arXiv:1807.02101 [hep-ph].
7. A. Bacchetta, V. Bertone, C. Bissolotti, G. Bozzi, F. Delcarro, F. Piacenza and M. Radici, *JHEP* **07**, 117 (2020), arXiv:1912.07550 [hep-ph].
8. A. Bermudez Martinez *et al.*, *Eur. Phys. J. C* **80**, 598 (2020), arXiv:2001.06488 [hep-ph].
9. R. P. Kauffman, *Phys. Rev. D* **44**, 1415 (1991).
10. D. Gutierrez-Reyes, S. Leal-Gomez, I. Scimemi and A. Vladimirov, *JHEP* **11**, 121 (2019), arXiv:1907.03780 [hep-ph].
11. D. Boer, W. J. den Dunnen, C. Pisano, M. Schlegel and W. Vogelsang, *Phys. Rev. Lett.* **108**, 032002 (2012), arXiv:1109.1444 [hep-ph].
12. D. Boer and C. Pisano, *Phys. Rev. D* **91**, 074024 (2015), arXiv:1412.5556 [hep-ph].
13. J. C. Collins, D. E. Soper and G. F. Sterman, *Nucl. Phys. B* **308**, 833 (1988).
14. D. Boer, *Few Body Syst.* **58**, 32 (2017), arXiv:1611.06089 [hep-ph].
15. G. T. Bodwin, E. Braaten and G. P. Lepage, *Phys. Rev. D* **51**, 1125 (1995), arXiv:hep-ph/9407339, [Erratum: Phys.Rev.D 55, 5853 (1997)].
16. M. G. Echevarria, *JHEP* **10**, 144 (2019), arXiv:1907.06494 [hep-ph].
17. J. C. Collins and D. E. Soper, *Nucl. Phys. B* **197**, 446 (1982).
18. D. Boer and W. J. den Dunnen, *Nucl. Phys. B* **886**, 421 (2014), arXiv:1404.6753 [hep-ph].
19. P. Sun, C. P. Yuan and F. Yuan, *Phys. Rev. D* **88**, 054008 (2013), arXiv:1210.3432 [hep-ph].
20. M. G. Echevarria, T. Kasemets, J.-P. Lansberg, C. Pisano and A. Signori, *Phys. Lett. B* **781**, 161 (2018), arXiv:1801.01480 [hep-ph].
21. J. C. Collins and D. E. Soper, *Nucl. Phys. B* **193**, 381 (1981), [Erratum: Nucl.Phys.B 213, 545 (1983)].
22. J. Bor and D. Boer, *Phys. Rev. D* **106**, 014030 (2022), arXiv:2204.01527 [hep-ph].
23. S. M. Aybat and T. C. Rogers, *Phys. Rev. D* **83**, 114042 (2011), arXiv:1101.5057 [hep-ph].
24. A. Bacchetta, F. G. Celiberto, M. Radici and P. Taels, *Eur. Phys. J. C* **80**, 733 (2020), arXiv:2005.02288 [hep-ph].
25. D. Chakrabarti, P. Choudhary, B. Gurjar, R. Kishore, T. Maji, C. Mondal and A. Mukherjee, *Phys. Rev. D* **108**, 014009 (2023), arXiv:2304.09908 [hep-ph].
26. A. Bacchetta, F. G. Celiberto and M. Radici, *Eur. Phys. J. C* **84**, 576 (2024), arXiv:2402.17556 [hep-ph].
27. BLFQ Collaboration, H. Yu, Z. Hu, S. Xu, C. Mondal, X. Zhao and J. P. Vary, *Phys. Lett. B* **855**, 138831 (2024), arXiv:2403.06125 [hep-ph].
28. A. Bacchetta, F. G. Celiberto, M. Radici and A. Signori, *Phenomenology of gluon TMDs from $\eta_{b,c}$ production*, in *29th International Workshop on Deep-Inelastic Scattering and Related Subjects*, (8 2022). arXiv:2208.06252 [hep-ph].
29. W. Lucha, F. F. Schoberl and D. Gromes, *Phys. Rept.* **200**, 127 (1991).
30. E. J. Eichten and C. Quigg, *Phys. Rev. D* **52**, 1726 (1995), arXiv:hep-ph/9503356.
31. G. P. Lepage, L. Magnea, C. Nakhleh, U. Magnea and K. Hornbostel, *Phys. Rev. D* **46**, 4052 (1992), arXiv:hep-lat/9205007.
32. P. L. Cho and A. K. Leibovich, *Phys. Rev. D* **53**, 150 (1996), arXiv:hep-ph/9505329.
33. J. H. Kuhn, J. Kaplan and E. G. O. Safiani, *Nucl. Phys. B* **157**, 125 (1979).
34. R. Gastmans, W. Troost and T. T. Wu, *Phys. Lett. B* **184**, 257 (1987).
35. P. L. Cho and A. K. Leibovich, *Phys. Rev. D* **53**, 6203 (1996), arXiv:hep-ph/9511315.

36. PHENIX Collaboration, A. Adare *et al.*, *Phys. Rev. D* **85**, 092004 (2012), arXiv:1105.1966 [hep-ex].
37. PHENIX Collaboration, A. Adare *et al.*, *Phys. Rev. Lett.* **98**, 232002 (2007), arXiv:hep-ex/0611020.
38. STAR Collaboration, B. I. Abelev *et al.*, *Phys. Rev. C* **80**, 041902 (2009), arXiv:0904.0439 [nucl-ex].
39. PHENIX Collaboration, A. Adare *et al.*, *Phys. Rev. D* **82**, 012001 (2010), arXiv:0912.2082 [hep-ex].
40. LHCb Collaboration, R. Aaij *et al.*, *Eur. Phys. J. C* **75**, 311 (2015), arXiv:1409.3612 [hep-ex].
41. LHCb Collaboration, R. Aaij *et al.*, *Eur. Phys. J. C* **80**, 191 (2020), arXiv:1911.03326 [hep-ex].
42. M. Butenschoen, Z.-G. He and B. A. Kniehl, *Phys. Rev. Lett.* **114**, 092004 (2015), arXiv:1411.5287 [hep-ph].
43. I. Babiarz, R. Pasechnik, W. Schäfer and A. Szczurek, *JHEP* **02**, 037 (2020), arXiv:1911.03403 [hep-ph].
44. A. V. Anufriev and V. A. Saleev, *Phys. Part. Nucl.* **55**, 836 (2024).
45. T. Hahn, *Comput. Phys. Commun.* **168**, 78 (2005), arXiv:hep-ph/0404043.
46. A. D. Martin, W. J. Stirling, R. S. Thorne and G. Watt, *Eur. Phys. J. C* **63**, 189 (2009), arXiv:0901.0002 [hep-ph].
47. Particle Data Group Collaboration, P. A. Zyla *et al.*, *PTEP* **2020**, 083C01 (2020).
48. E. Braaten, B. A. Kniehl and J. Lee, *Phys. Rev. D* **62**, 094005 (2000), arXiv:hep-ph/9911436.
49. A. Arbuzov *et al.*, *Prog. Part. Nucl. Phys.* **119**, 103858 (2021), arXiv:2011.15005 [hep-ex].
50. J. P. Lansberg *et al.*, *PoS* **ICHEP2012**, 547 (2013), arXiv:1212.3450 [hep-ex].
51. A. A. Chernyshev and V. A. Saleev, *Phys. Rev. D* **106**, 114006 (2022), arXiv:2211.07989 [hep-ph].
52. STAR Collaboration, J. Adam *et al.*, *Phys. Lett. B* **786**, 87 (2018), arXiv:1805.03745 [hep-ex].
53. M. Beneke, M. Kramer and M. Vanttinen, *Phys. Rev. D* **57**, 4258 (1998), arXiv:hep-ph/9709376.
54. B. A. Kniehl and J. Lee, *Phys. Rev. D* **62**, 114027 (2000), arXiv:hep-ph/0007292.